Comparison of Plasma and Laser Beam Welding of Steel Sheets Treated by Nitrooxidation

Ivan Michalec, Milan Marônek

Department of Welding
Faculty of Materials Science and Technology in Trnava
J. Bottu 25, 917 24 Trnava, Slovakia
e-mail: ivan.michalec@stuba.sk, milan.maronek@stuba.sk

Abstract: Steel sheets treated by nitrooxidation in comparison to material without surface treatment are characterized by increased mechanical properties and enhanced corrosion resistance. The paper deals with the comparison of solid-state laser beam welding and plasma arc welding in order to reduce the high initial costs of laser beam equipment and to find an adequate counterpart from the arc welding sphere. Results prove solid-state laser beam welding is the most suitable welding method for welding of this type of treated steels, although plasma arc welding, especially after parameters optimizing, can be an adequate alternative to laser beam welding.

Keywords: nitrooxidation; plasma arc welding; laser beam welding

1 Introduction

In view of the positive influence on the steel sheet, a surface treatment is one of the most monitored parts in the industry [1, 2]. The process of nitrooxidation, consisting of a surface nitridation with subsequent oxidation, is a part of non-conventional surface treatment methods, by which a radical mechanical properties increase (Tensile Strength, Yield Strength), together with an increase in the corrosion resistance up to level 10, can be achieved [3]. However, it is not always possible to apply the treatment as the final operation, and materials should be welded after the treatment. In such cases, the knowledge of suitable welding methods that have the least deterioration effect on the surface is essential [1, 2, 4].

In previous outcomes [3, 4, 5, 6], various arc and beam welding methods were examined. In almost every welding method, a high level of porosity together with spatter and weld bead irregularities were observed [7]. Only the joints welded by solid-state laser beam welding were defects-free, and the joints had superior quality and good consistency [3, 9]. Nevertheless, the high initial cost of the laser equipment turned attention towards an appropriate arc method. The only arc method not tested was plasma arc welding and was supposed as an adequate option to laser beam welding.

2 Materials and Methods Used for Experiments

For all the experiments, low carbon deep drawing steel DC 01 EN 10130/91 of 1 mm in thickness was used. The chemical composition of steel DC 01 is referred to in Table 1.

Table 1
Chemical composition of steel DC 01 EN 10130/91

EN designation	C [%]	Mn [%]	P [%]	S [%]	Si [%]	Al [%]
DC 01 10130/91	**0.10**	**0.45**	**0.03**	**0.03**	**0.01**	**-**

2.1 Thermo-Chemical Treatment

The material was consequently treated by the process of nitrooxidation in a fluidized bed. The nitridation fluid environment was Al_2O_3 with granularity of 120 μm. The fluid environment was wafted by gaseous ammonia. Oxidation was subsequently carried out in the vapours of distilled water. The process parameters are presented in Table 2.

Table 2
Process of nitrooxidation parameters

	Nitridation	Oxidation
Time [min]	**45**	**5**
Temperature [°C]	**580**	**380**

2.2 Methods Used for Experiments

Specimens welded by plasma arc welding (PAW) were made with a Fronius MagicWave 2200 machine with integrated PlasmaModule 10 in Fronius Slovakia, Trnava. Argon with a purity of 99.996 % was used as the shielding gas as well as the plasma gas. The samples were welded in continual and pulse mode, respectively. To provide the constant gap between welded materials, steel sheets were stitched together by GTAW. The fixation of the welded materials during welding is shown in Fig. 1.

Figure 1
Plasma arc welding configuration

Specimens welded by a solid-state laser beam welding (LBW) were welded with a TruDisk 1000 laser machine in PGS Automation, Trnava. The welding parameters are presented in Table 3. The welding process is shown in Fig. 2.

Table 3
TruDisk 1000 laser source characteristics

Source type	TruDisk 1000
Power	1000 W
Optics	ϕ 35 mm
Focal length	200 mm
Focusing plane	surface
Collimation length	100 mm
Spot size	600 μm
Wavelength	1030 nm
Welding speed	20 mm/s
Shielding gas	Argon (10 l/min)
Optical cable	Step Index Φ 300 μm

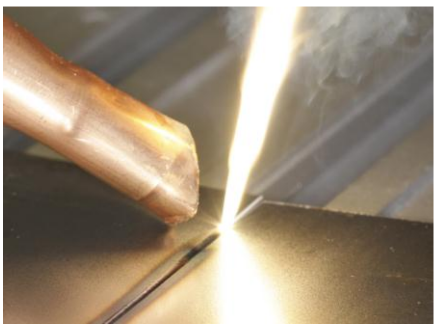

Figure 2
Solid-state laser beam welding process

Scanning electron microscopy analysis, microhardness measurements, the Erichsen cupping test, and tensile tests were performed in order to obtain the complex information about the properties of the material treated by nitrooxidation.

The weld joints were evaluated by macroscopic and microscopic analysis, microhardness measurements, the Erichsen cupping test and tensile tests. The results of both welding methods were compared and assessed.

3 Results

3.1 Material Properties

The key parameters during the nitridation and oxidation phase of the process are temperature and time. The final material properties thus depend on them, and they indirectly effect the welding process stability and weld joint quality. The knowledge of the material properties was therefore seen as essential.

3.1.1 Microscopic Analysis

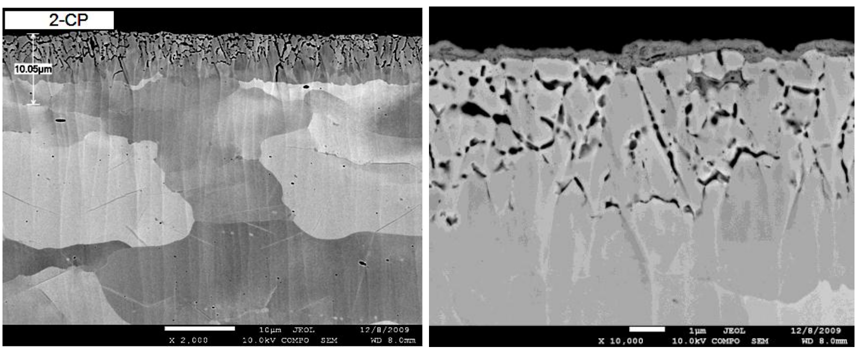

a) b)

Figure 3

Surface layer of the base material after the nitrooxidation process

a) overall view; b) close up view on the oxide and ε-phase layers

Microscopic analysis was performed with a JEOL 7600-F scanning electron microscope. The microstructure of the base material was ferritic with the dominant orientation of the grains as a consequence of the rolling process. The nitrooxidized surface layer (Fig. 3a) consisted of a very thin oxide layer with thickness up to 700 nm (Fig. 3b). Under the oxide layer, a continuous layer of the ε-phase (Fig. 3b), composed of $Fe_{2\text{-}3}N$, was observed. This layer had a thickness of approx. 10 μm. Beneath the ε-phase layer, a 60 μm thick compound layer was identified. It consisted of a ferritic matrix and precipitated needle shaped nitrides Fe_4N.

3.1.2 Tensile Tests

The mechanical properties of the material were obtained by tensile tests in accordance to STN EN 10002-1. The average results from five measurements are documented in Table 4.

Table 4

Results obtained by tensile tests

DC 01 EN 10130/91	Yield Strength [MPa]	Tensile Strength [MPa]
Before nitrooxidation	**200**	**270**
After nitrooxidation	**310**	**380**

After the process of nitrooxidation, increases in Yield Strength by 55% and in Tensile Strength by 40% were observed.

3.1.3 Corrosion Test

The corrosion test was carried out in a condensation chamber KB 300 type 43096101 in 100% moisture (environment of distilled water). The testing samples were consequently analysed after 16, 48, 72, 144 and 240 hours and assessed by gravimetric analysis. The results are documented in Table 5.

Table 5

The gravimetric analysis results

Material DC 01 EN 10130/91	Exposure in condensation chamber [h]				
	16	48	72	144	240
	Mass increase [g/m^2]				
Before nitrooxidation	**0.051**	**0.180**	**0.638**	**6.992**	**8.490**
After nitrooxidation	**0.076**	**0.083**	**0.109**	**0.124**	**0.128**

Based on the results, material DC 01 after the process of nitrooxidation was classified as having the maximal (level 10) resistance to atmospheric corrosion. Only 0.128 g/m^2 of mass increase was observed after 240 hours in the condensation chamber. This was more than 66 times less in comparison to the material without nitrooxidation.

3.1.3 Microhardness Measurements

The results of microhardness testing according to Vickers, measured across the material thickness, are documented in Fig. 4. A Buehler IndentaMet 1100 Series tester was used as the measuring equipment. The force load was F = 0. 981 N (m = 100 g) and the loading time was t = 10 s. To acquire the most accurate results, the measurements were repeated three times in different places. Fig. 4 shows an increase in microhardness of more than 47% at the depth of 60 μm from the material's surface. Likewise, it can be stated that the material was affected by the nitrooxidation to the depth of 350 – 400 μm from the surface. However, the microhardness values in the area of ε-phase, where the highest values were expected, could not be obtained due to measuring equipment limitations.

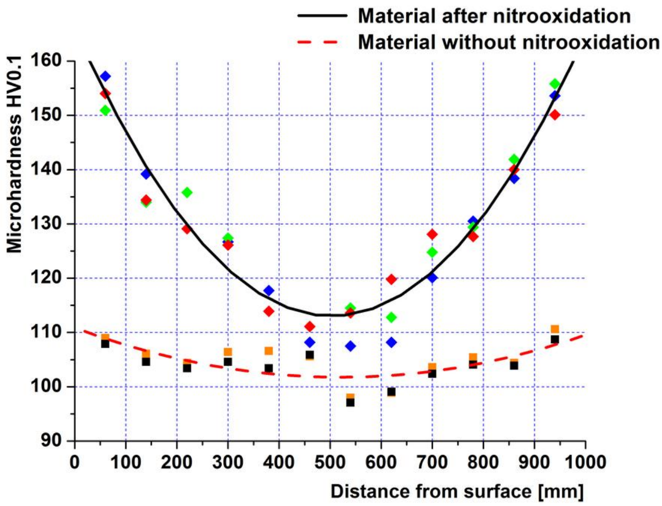

Figure 4
Microhardness trend comparison

3.1.4 Erichsen Cupping Test

An Erichsen cupping test was performed in order to evaluate the forming properties of nitrooxidized material with regard to the influence of the surface layer on deep drawability of the steel. After the process of nitrooxidation, the depth of the indent decreased by 10% in comparison to untreated material. Based on this, the material treated by nitrooxidation loses its deep-drawability, although it is still suitable for forming operations. On the other hand, the character of the fracture corresponded to the untreated material. The result of the Erichsen cupping test is documented in Fig. 5.

Figure 5
Sample after the Erichsen cupping test with close-up view on transverse fracture

3.2 Joints Properties

There are many factors having a direct and indirect influence on weld joint quality. In order to get the maximum available information concerning the weld joint quality, several analyses were carried out.

3.2.1 Visual Inspection

The visual inspection results of the joints welded by a LBW and PAW are shown in Fig. 6. The PAW joints (Fig. 6a) were about 50% wider than those welded by LBW (Fig. 6b).

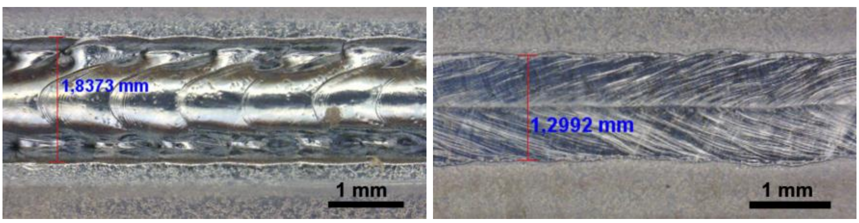

a) b)

Figure 6
Visual inspection of the joints (face side of the joints)
a) plasma arc welding; b) solid-state laser beam welding

3.2.2 Macroscopic Analysis

The macroscopic analysis (Fig. 7) revealed that the joints welded by PAW (Fig. 7a) had no porosity, which was the main issue in almost every arc welding method [8]. Nevertheless, the presence of the undercuts, situated along the joint's length, were inappropriate. Figure 7 revealed a more than three times wider Heat Affected Zone (HAZ) than in the joints made by LBW.

The joints welded by LBW welding (Fig. 7b) had a superior quality, very narrow HAZ and were defects-free. The joints had appropriate shape with no bead reinforcement.

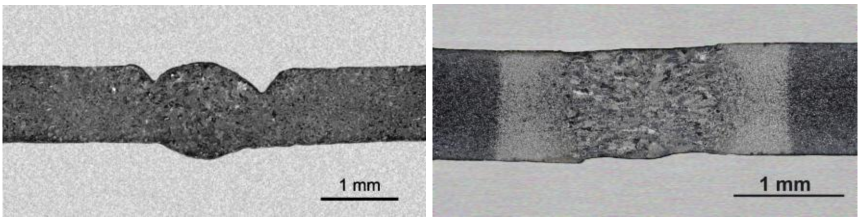

a) b)

Figure 7
Macroscopy of the joints
a) plasma arc welding; b) solid-state laser beam welding

3.2.3 Microscopic Analysis

The microscopic analysis was primarily focused on the Weld Metal (WM) and HAZ area. The results of the microscopic analysis of the joints welded by PAW are shown in Fig. 8. The microstructure of WM was ferritic, mainly composed of coarse-grained acicular ferrite. The polygonal ferrite was observed in a minor amount. The HAZ consisted of polygonal ferrite with a visible fine-grained structure.

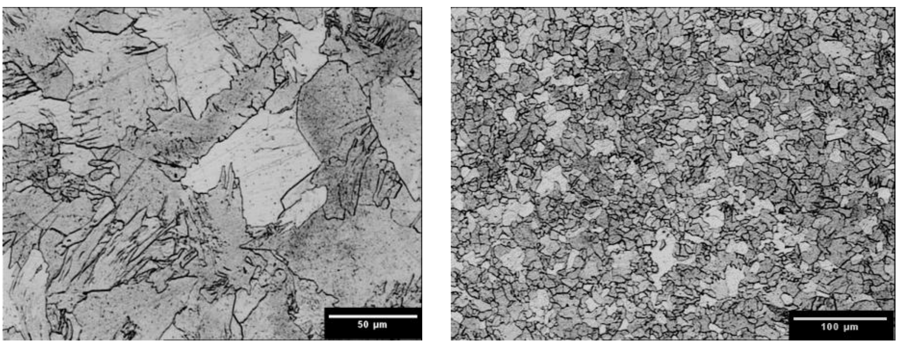

a) b)

Figure 8
Microscopic analysis of the plasma arc welding joints
a) Weld Metal; b) Heat Affected Zone

The results of microscopic analysis of the joints welded by LBW are presented in Fig. 9. The WM was created primarily by the acicular ferrite and the ferrite precipitated along to columnar grains. The composition of HAZ corresponded to the PAW joints.

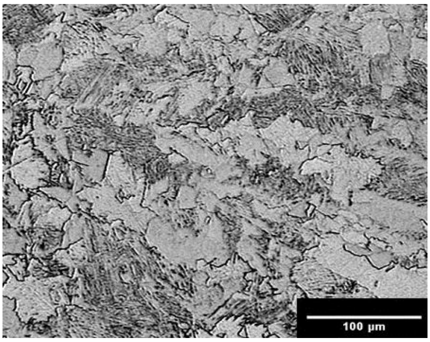

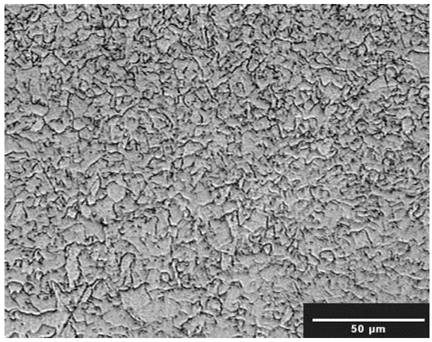

a) b)

Figure 9
Microscopic analysis of the laser beam welding joints
a) Weld Metal; b) Heat Affected Zone

3.2.4 Microhardness Measurements

Microhardness measurements of the joints were carried out in the same way as in the case of the material's examination. Typical microhardness trends are illustrated in Fig 10. The highest microhardness values were observed in WM and the lowest in the BM. The microhardness of HAZ and BM was comparable in both welding methods. The much higher values in the WM area (more than 30%) were obtained in the PAW.

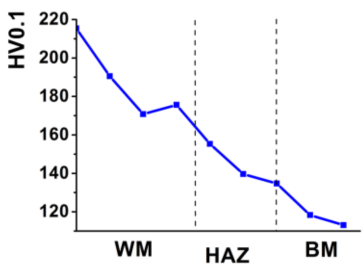

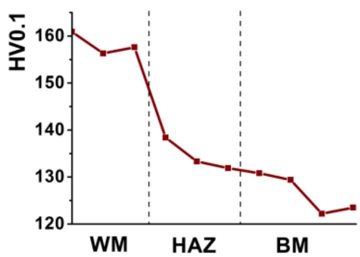

a) b)

Figure 10
Microhardness trend of the joints
a) plasma arc welded; b) solid-state laser beam welded

3.2.5 Tensile Tests

The tensile tests were accomplished on samples with the dimensions of 200×20×1 mm with the weld in the middle of the sample. As the testing device, a tensile test EU 40 machine was used. The results (Fig. 11) showed that both PAW and the LBW joints were fractured outside the joint area and thus marked as suitable.

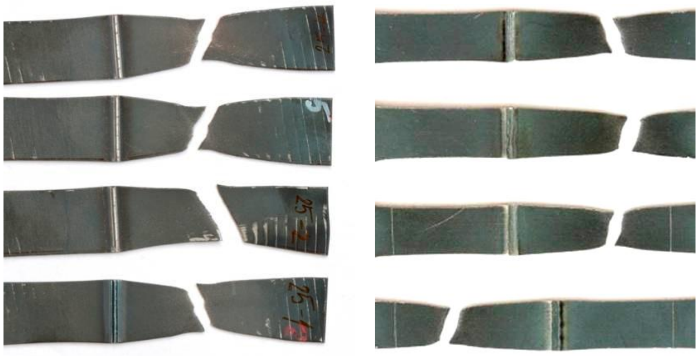

a) b)

Figure 11

Samples after the tensile tests

a) plasma arc welded; b) solid-state laser beam welded

3.2.6 Erichsen Cupping Test

The Erichsen cupping test was carried out in accordance to STN EN 1001-5. The dimension of the samples was 250×50×1 mm. The results of the samples are documented in Fig. 12. Figure 12 shows that in both PAW (Fig. 12a) and LBW joints (Fig. 12b) the transverse type of fracture was observed in every sample, which confirmed the good mechanical properties of the joints, since the fracture did not occur along the joint.

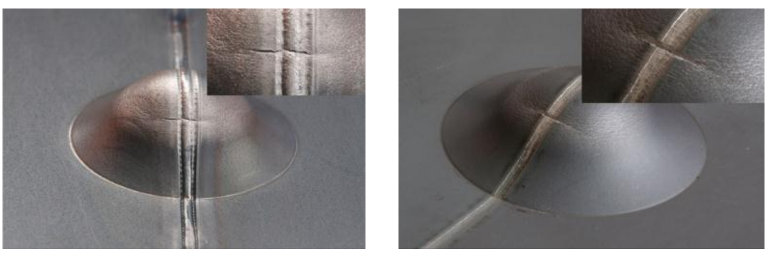

a) b)

Figure 12

Samples after the Erichsen cupping test a with close-up view on the transverse fracture

a) plasma arc welding; b) solid-state laser beam welding

The results of the deep-drawability measurements by the Erichsen cupping test are shown in Table 6. The PAW joints exhibited an increase in the depth indent by more than 11% in comparison to LBW joints.

Table 6
Depths of indent in the Erichsen cupping test

	Plasma arc welding	Solid-state laser beam welding
Specimen No.	Depth of indent	
1	**9.20**	**8.10**
2	**9.10**	**8.10**
3	**8.85**	**8.00**

4 Discussion

The comparison of the joints' widths uncovered a wider joint in PAW, by more than 50%. Likewise, the macroscopic analysis proved a three-times-wider HAZ in PAW joints. This was caused by the higher thermal density of the laser beam distributed into the narrower surface in comparison to plasma arc welding.

The LBW joints had more consistent microhardness trend along the measured length, whereas the PAW joints exhibited a continuous decrease of the microhardness towards the base material. It gave the evidence of microstructure homogeneity across the weld joint, whereas the microstructure of PAW joints was more heterogeneous.

Even though undercuts were observed in the PAW joints, the tensile tests as well as the Erichsen cupping tests proved the good mechanical properties of the joints. Nevertheless, the presence of undercuts indicates that the process parameters need optimizing.

The Erichsen cupping test proved the lower depth of indent in the case of the LBW joints, although the microhardness measurements showed lower microhardness values. These results did not correspond to the expectations of the comparable cupping index and they should be verified in further research.

Conclusion

The material treated after the process of nitrooxidation in the fluidized bed and its welding by solid-state laser beam welding as well as plasma arc welding were analysed. In the surface layer, the individual layers were identified. Likewise, the mechanical properties together with the corrosion resistance increase were documented. The material after nitrooxidation treatment loses its deep-drawability, but on the other hand, it keeps the ability to be formed.

The tests on joints welded by laser proved excellent results. The visual inspection of the joints welded by plasma arc revealed a significant presence of undercuts, whereas the macroscopic analysis confirmed the absence of porosity in the weld joint. Based on the results, there is an assumption that plasma arc welding could have a potential to become an alternative welding method to the laser beam welding of steel sheets treated by nitrooxidation.

Further research activity will be focused on the optimization of the plasma arc welding parameters. The plasma and shielding gas flow rate, the torch angle and the electrode stickout will be taken into account.

Acknowledgements

This paper was prepared within the support of Slovak Research and Development Agency, grant No. 0057-07 and Scientific Grant Agency, grant No. 1/0203/11.

References

[1] Michalec, I.: CMT Technology Exploitation for Welding of Steel Sheets Treated by Nitrooxidation. Diploma thesis, Trnava 2010

[2] Michalec, I., et. al.: Metallurgical Joining of Steel Sheets Treated by Nitrooxidation by a Hybrid CMT - Laser Process, 20th Anniversary International Conference on Metallurgy and Materials, May 18-20, 2011, Brno, Czech Republic

[3] Bárta, J.: Welding of Special Treated Thin Steel Sheets: Dissertation thesis, Trnava, 2010

[4] Marônek, M. et. al.: Laser Beam Welding of Steel Sheets Treated by Nitrooxidation, 61st Annual Assembly and International Conference of the International Institute of Welding, Graz, Austria, 6-11 July 2008

[5] Lazar, R., Marônek, M., Dománková, M.: Low Carbon Steel Sheets Treated by Nitrooxidation Process, Engineering Extra, 2007, No. 4, p. 86

[6] Marônek, M. et. al.: Comparison of Laser and Electron Beam Welding of Steel Sheets Treated by Nitrooxidation, Congresso da ABM (CD-ROM). - ISSN 1516-392X. - 65th ABM international Congress. 18th IFHTSE Congress. 1st TMS/ABM : Brazil, Rio de Janeiro, July 26-30, 2010

[7] Bárta, J. et al.: Joining of Thin Steel Sheets Treated by Nitrooxidation, Proceeding of Lectures of 15th Seminary of ESAB + MTF-STU in the scope of seminars about welding and weldability. Trnava, AlumniPress, 2011, pp. 57-67

[8] Marônek, M. et al.: Welding of Steel Sheets Treated by Nitrooxidation, JOM-16: 16th International Conference on the Joining of Materials & 7th International Conference on Education in Welding ICEW-7, May 10-13, Tisvildeleje, Denmark, ISBN 87-89582-19-5

[9] Viňáš, J.: Quality Evaluation of Laser Welded Sheets for Cars Body. In: Mat/tech automobilového priemyslu: Zborník prác vt-seminára s medzinárodnou účasťou : Košice, 25.11.2005. Košice: TU, 2005. pp. 119-124. ISBN 80-8073-400-3